

Study of Low Resistivity and High Work Function ITO Films Prepared by Oxygen Flow Rates and N₂O Plasma Treatment for Amorphous/Crystalline Silicon Heterojunction Solar Cells

Shahzada Qamar Hussain^{1,3}, Woong-Kyo Oh², Sunbo Kim¹, Shihyun Ahn², Anh Huy Tuan Le², Hyeongsik Park², Youngseok Lee¹, Vinh Ai Dao², S. Velumani², and Junsin Yi^{1,2,*}

¹Department of Energy Science, Sungkyunkwan University, Suwon, 440-746, Republic of Korea

²College of Information and Communication Engineering, Sungkyunkwan University, Suwon, 440-746, Republic of Korea

³Department of Physics, COMSATS Institute of Information Technology, Lahore, 54000, Pakistan

Pulsed DC magnetron sputtered indium tin oxide (ITO) films deposited on glass substrates with lowest resistivity of $2.62 \times 10^{-4} \Omega \cdot \text{cm}$ and high transmittance of about 89% in the visible wavelength region. We report the enhancement of ITO work function (Φ_{ITO}) by the variation of oxygen (O₂) flow rate and N₂O surface plasma treatment. The Φ_{ITO} increased from 4.43 to 4.56 eV with the increase in O₂ flow rate from 0 to 4 sccm while surface treatment of N₂O plasma further enhanced the ITO work function to 4.65 eV. The crystallinity of the ITO films improved with increasing O₂ flow rate, as revealed by XRD analysis. The ITO work function was increased by the interfacial dipole resulting from the surface rich in O⁻ ions and by the dipole moment formed at the ITO surface during N₂O plasma treatment. The ITO films with high work functions can be used to modify the front barrier height in heterojunction with intrinsic thin layer (HIT) solar cells.

Keywords: ITO Films, N₂O Plasma Treatment, XPS, Work Function, Barrier Height, HIT Solar Cell.

1. INTRODUCTION

The high efficiency HIT solar cell is considered a unique future photo-voltaic device due to its low cost, low temperature hydrogenated amorphous silicon (a-Si:H) deposition, and stability of crystalline silicon (c-Si). Indium tin oxide (ITO) films are commonly used as transparent anti-reflection electrodes in organic light-emitting devices (OLEDs), flat panel displays and solar cells due to their low resistivity, high transmittance in the visible wavelength region and wide optical bandgap.^{1,2} In HIT solar cell, the ITO films are used as an anode to inject holes into the highest occupied molecular orbital (HOMO) of the a-Si:H(p) layer. A change in work function of the ITO films affects the hole carrier injection flow into the ITO/a-Si:H(p) interface, that plays a critical role in key

device parameters such as operating voltage. Therefore, ITO films with low resistivity, high transmittance and high work function are required to improve the performance of the HIT solar cell.^{3,4}

The work function of ITO films has been enhanced by methods mainly related to surface cleaning. The Φ_{ITO} can be influenced by the chemical composition of ITO films, as reported by Meson and Kim et al.^{5,6} Surface treatment of ITO films using various plasma or UV ozone can remarkably increase the ITO work function and enhance the hole-injection efficiency and device reliability.^{3,7,8} The Φ_{ITO} can be enhanced by IR irradiation or by changing the substrate temperature (T_s), as reported by Park, Nakasa and Oh et al.⁹⁻¹¹ Recently, Ahn, Hussain and Lee et al. reported the experimental enhancement of the ITO work function for the application of HIT solar cells.^{2,4,12,13} Few simulation studies related to the Φ_{ITO} were performed to

* Author to whom correspondence should be addressed.

improve the performance of HIT solar cells.^{1, 14, 15} However, the enhancement of Φ_{ITO} affects the resistivity or transmittance of ITO films, so films with low resistivity, high transmittance and high work function are difficult to obtain. It has been founded that Φ_{ITO} can vary from 4.3 to 5.1 eV depending on the stoichiometry of ITO films, organic contamination and oxidation type.^{16, 17} Among the several reports related to the enhancement of Φ_{ITO} , only few have dealt with pulsed DC magnetron sputtered ITO films of low resistivity, high transmittance and high work function for the HIT solar cell.

In this paper, we report the influences of O_2 flow rate and N_2O plasma treatment on the work function of pulsed DC magnetron sputtered ITO films. The behavior of ITO work function is explained by the X-rays photoelectron spectroscopic (XPS) analysis. The electrical, structural and optical properties of the ITO films are explained for various O_2 flow rates and N_2O plasma treatment. The influence of the ITO work function on the front contact barrier height of the HIT solar cell is also explained.

2. EXPERIMENTAL DETAILS

ITO films were deposited on silicon wafers and glass (eagle 2000, Corning) substrates by using a pulsed DC magnetron sputtering. The silicon wafers and the glass substrates were cleaned in acetone followed by methyl alcohol for 10 min and then rinsed with D.I water. The ITO target for the sputter deposition was composed of 90 wt% In_2O_3 and 10 wt% SnO_2 with 99.999% purity. Argon gas of 20 sccm was used in the sputtering process, and O_2 flow rate was varied from 0 to 0.4 sccm. The thickness of all ITO films was fixed to 100 ± 5 nm. The base pressure of the chamber was maintained up to 1×10^{-5} Torr and the working pressure was 3×10^{-3} Torr. N_2O gas plasma treatment of the as deposited ITO films was carried out. The samples were biased by RF power to generate the plasma.

Spectroscopic ellipsometry (Nano-view, SE MF-1000) was used to measure the thickness and refractive index of the deposited ITO films. The electrical properties, such as the carrier concentration (n), resistivity (ρ) and Hall mobility (μ) of the ITO films were characterized by a Hall Effect measurement (Ecopia HMS-3000) system with 1 mA current and magnetic field of 0.51 Tesla. The structural properties of the ITO films were analyzed by X-ray diffractometry (XRD, Panalytical PW 3060) using CuK_α radiation ($\lambda = 0.1541$ nm). The X-rays photoelectron spectroscopic (XPS) system with monochromatic Al K_α (1486.6 eV) source was used to measure the work function and atomic concentration of the ITO films. The optical transmittances of the ITO films were characterized by a UV-Vis spectrophotometer (SCINCO S-3100) at room temperature. A simulation study was performed to draw the band diagram of the front contact barrier height of the HIT solar cell.

3. RESULTS AND DISCUSSION

Figure 1 shows the X-rays photoelectron spectroscopic (XPS) spectra of ITO films deposited under various O_2 flow rates and N_2O plasma treatment. The ITO work function derived from the XPS data, increased from 4.43 to 4.56 with increasing O_2 flow rate from 0 to 0.4 sccm.¹⁸ The ITO work function was further enhanced from 4.56 eV by N_2O surface plasma treatment. The oxidative treatments incorporated more oxygen into the ITO surface, improving the work function, as reported by Meson et al.⁵ The increase of Φ_{ITO} is attributed to the interfacial dipole caused by a surface rich in negatively charged oxygen.^{3, 5} With N_2O surface plasma treatment, the number of O—O bonds increased due to the adsorption of oxygen ions at the surface of the ITO films. These O—O bonds created a dipole layer of O^- ions and hence a dipole moment formed at the ITO surface, increasing Φ_{ITO} .^{3, 22} The O^- ions formed on the surfaces of the ITO films prepared by O_2 and N_2O plasma treatments can repel the free electrons in the conduction band, shifting the surface Fermi level. This Fermi level shift towards the middle of the band gap can lead to the reduction of the hole potential barrier at the ITO/a-Si:H(p) interface of the HIT solar cell. The more the O^- ions adsorbed on the ITO surface, the higher the Φ_{ITO} during N_2O plasma treatment. The more adsorbed O^- ions induce a high dipole moment on the ITO surface during N_2O plasma treatment, reducing the potential at the front ITO/a-Si:H(p) interface of the HIT solar cell. ITO films with high Φ_{ITO} are used to inject holes in the front contact barrier height of the ITO/a-Si:H (p) interface in the HIT solar cell.^{4, 12–15}

Figure 2 shows the XPS spectra of the ITO films prepared under various O_2 flow rates and N_2O plasma treatment. As shown in Figure 2(a), the decrease in the intensity of C 1s was ascribed to the increase in O_2 flow rate and N_2O plasma treatment. The carbon atoms were removed from the ITO surface as a result of mixing with the gas radicals present in the plasma during the sputtering process. The intensity of O 1s shown in Figure 2(b)

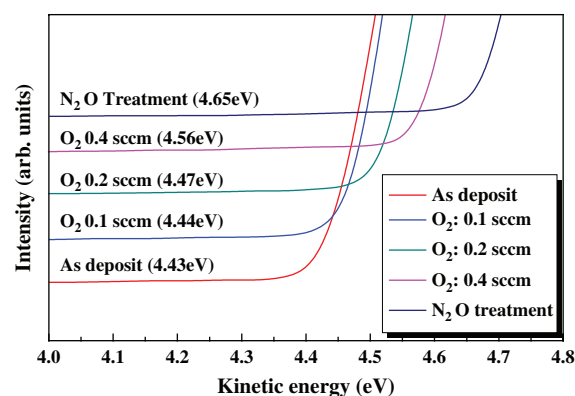


Figure 1. Typical XPS spectra of ITO films with various O_2 flow rates and N_2O surface plasma treatment.

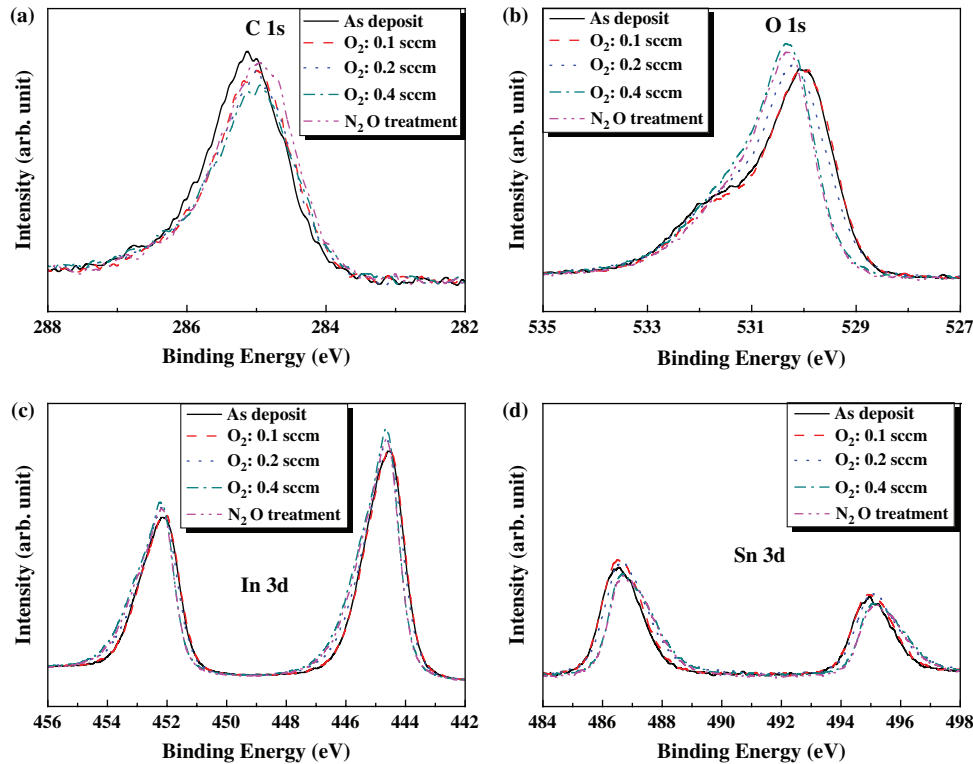


Figure 2. The XPS spectra of (a) C 1s, (b) O 1s, (c) In 3d and (d) Sn 3d core levels of ITO films prepared with various O₂ flow rates and with N₂O plasma treatment.

increased with the increase in O₂ flow rate and N₂O plasma treatment. The broadening of the O 1s peak for the 0.4 sccm O₂ case and the N₂O plasma treatment case at the higher binding energy side indicate the O—O bonds of the O⁻ ions adsorbed on the surfaces of the corresponding ITO films. Figure 2(c) presents the intensity of the In 3d peak, which slightly increases with O₂ flow rate and N₂O plasma treatment due to the increased oxidation. The intensity of the Sn 3d peak is shown in Figure 2(d). The intensity of the Sn 3d peak first increase and then decrease with the increase of O₂ flow rate and N₂O plasma treatment.^{3, 19, 20} The ITO work functions and the corresponding atomic concentrations (in percent) of In, Sn, O and C are shown in Table I.

The XRD patterns of the ITO films deposited at various O₂ flow rates are presented in Figure 3. All peaks were assigned to the cubic bixbite structure of In₂O₃. The (222) and (440) peaks are the most prominent, showing that the

ITO films had the (111) and (110) preferential orientations, regardless of O₂ flow rate. The oxygen vacancies in the ITO films deposited under Ar ambient gas play an important role in atomic diffusion: oxygen atoms can diffuse through these vacancies. Therefore, various preferred planes were formed in the argon sputtered ITO films.²³ The intensities of peaks (222) and (440) gradually decrease from 0 to 0.3 sccm and finally increase at 0.4 sccm oxygen flow rate. The additional peaks at (211), (400) and (622) indicate that the ITO films were fully stabilized and that the crystal orientation was influenced by O₂ flow rate.^{21, 22}

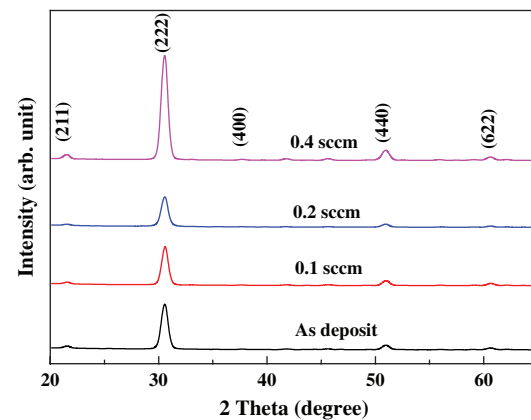


Figure 3. The X-ray diffraction (XRD) analysis of the ITO films as a function of O₂ flow rate.

Table I. ITO work function and atomic concentration C_x ($x = \text{In, Sn, O, C}$) measured by X-rays photoelectron Spectroscopy (XPS).

	Φ_{ITO} (eV)	C_{In} (%)	C_{Sn} (%)	C_{O} (%)	C_{C} (%)
0 sccm	4.43	29.32	3.37	47.52	19.79
0.1 sccm	4.44	32.42	3.64	46.97	18.98
0.2 sccm	4.47	30.54	3.59	47.48	18.39
0.4 sccm	4.56	31.50	3.32	46.79	18.39
N ₂ O plasma	4.65	30.87	3.39	46.04	19.70

Figure 4(a) shows the resistivity of the ITO films at various O_2 flow rates and N_2O plasma treatment. It can be seen that the resistivity slightly increases from 2.62×10^{-4} to $3.41 \times 10^{-4} \Omega \cdot \text{cm}$ as the O_2 flow rate increases from 0 to 0.4 sccm. The resistivity of the ITO film with N_2O plasma treatment was $3.43 \times 10^{-4} \Omega \cdot \text{cm}$. The slight increase in the resistivity was due to the additional oxygen flow during the sputtering process. It is well known that the resistivity of ITO films depends on the combined effect of Hall mobility and carrier concentration. The refractive index of ITO films gradually increases from 1.96 to 2.07 with increasing O_2 flow rate and N_2O plasma treatment (not shown). A high value of refractive index indicates very dense and crystalline films. The change in carrier concentration and hall mobility of the ITO thin films was the main reason for the increase in refractive index resulting in electron plasma wavelength movement.^{23,24} Figure 4(b) shows the Hall mobility and carrier concentration of the ITO films. The carrier concentration of the ITO films decreases with increasing O_2 flow rate and N_2O plasma treatment. The decrease in the carrier concentration of the ITO films from 8.86×10^{20} to $5.35 \times 10^{20} \text{ cm}^{-3}$ was due to the filling of the oxygen vacancies and deactivation of the donor. However, the Hall mobility increases from 26.8 to $33.37 \text{ cm}^2/\text{V} \cdot \text{s}$ as the O_2 gas rate increases from 0 to 0.4 sccm. It further increases to $34.12 \text{ cm}^2/\text{V} \cdot \text{s}$ with N_2O plasma treatment. Different types of electron scattering mechanisms like negative charged scattering, ionized impurity scattering and

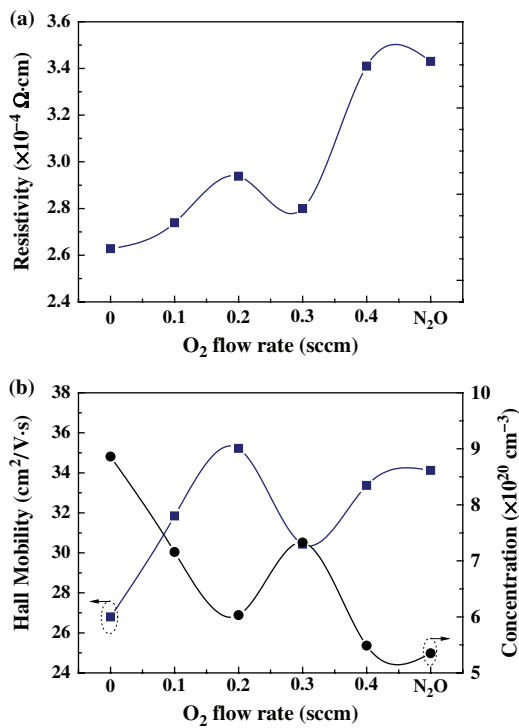


Figure 4. The electrical characteristics of (a) resistivity (b) Hall mobilities and carrier concentrations of the ITO films prepared with various O_2 flow rates and N_2O plasma treatment.

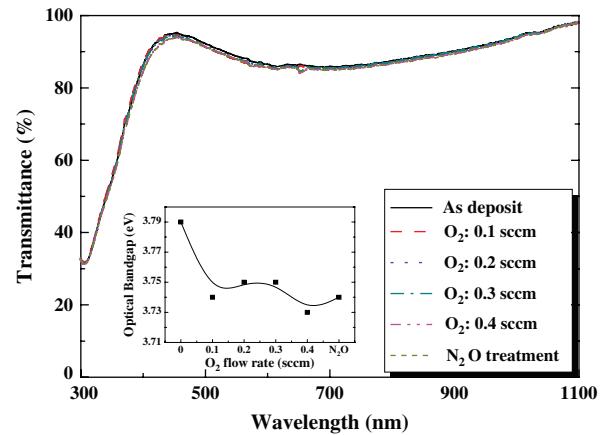


Figure 5. The optical transmittance of the ITO films prepared with various O_2 flow rates and N_2O plasma treatment. The optical bandgap of the ITO films is shown in the inset.

neutral defect scattering may be responsible for the change in the mobility.^{25,26}

The optical transmittance of the ITO films with increasing O_2 flow rate and N_2O plasma treatment is shown in Figure 5. The transmittance in the visible wavelength region decreases from 88.75 to 87.76% with increasing O_2 flow rate from 0.1 to 0.4 sccm and N_2O plasma treatment. A maximum transmission of about 88.29% was achieved in the visible (400–800) nm wavelength region by the ITO films deposited at 0.2 sccm O_2 flow rate. The average visible transmittance of all ITO films was 88%. The slight decrease in transmittance is mainly related to the decrease in carrier concentration of the ITO films. The optical bandgap of the ITO films decreased from 3.79 to 3.74 eV with increasing O_2 flow rate and N_2O plasma treatment. The decrease in carrier concentration and Burstein-Moss effect caused the reduction in the optical bandgap of the ITO films.^{19,27}

Figure 6 depicts the equilibrium band diagram of the front contact barrier height of the HIT solar cell as a

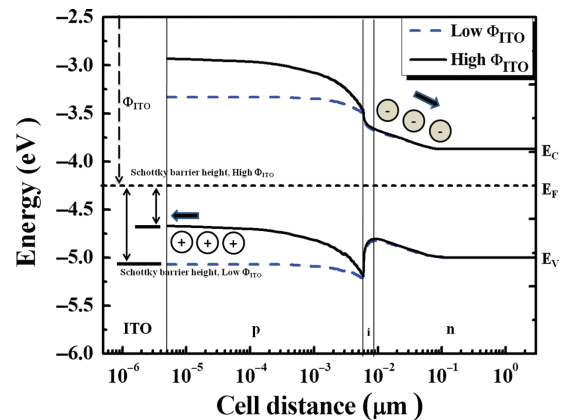


Figure 6. The band diagram of front contact barrier (ITO/a-Si:H(p)/a-Si:H(i)/c-Si(n)) height of HIT solar cell as a function of ITO work function.

function of ITO work function. The difference in the work function between the ITO and a-Si:H(p) layer was represented by the band bending in the a-Si:H(p) region. An electron injection barrier was developed due to lower Φ_{ITO} than that of the a-Si:H(p) layer, which limited the open circuit voltage (V_{oc}) downward band bending. The schottky barrier height of the ITO/a-Si:H(p) interface can be reduced by increasing the ITO work function, which promotes the migration of holes carriers from a-Si:H(p) layer to the ITO layer.^{2,4,12-15} Therefore, ITO films with low resistivity, high transmittance and work function can be used as anti-reflection layers for future high efficiency solar cell devices.

4. CONCLUSION

We reported ITO films with lowest resistivity of $2.62 \times 10^{-4} \Omega \cdot \text{cm}$, high visible transmittance of about 89% and work function of 4.65 eV by the O_2 flow rate and the N_2O surface plasma treatment. The ITO work function was enhanced from 4.43 to 4.65 eV with increasing O_2 flow rate from 0 to 0.4 sccm and with N_2O plasma treatment. The maximum work function of 4.65 eV was obtained by N_2O plasma treatment. The enhancement in Φ_{ITO} was mainly related to the presence of an interfacial dipole resulting from the surface rich in O^- ions. The more O^- ions adsorbed on the ITO surface during N_2O plasma treatment led to the high work function, rather than O_2 reactive sputtering. The ITO film showed higher degrees of crystallinity with increasing O_2 flow rate. The electrical resistivity of the film slightly increased when more O_2 was added during the sputtering process. However, the O_2 flow rate had an almost negligible influence on the optical transmittance of the ITO film. A highly conductive ITO films with high transmittance and work function are suitable for the improvement of performance in HIT solar cells.

Acknowledgments: This work was supported by the New and Renewable Energy Core Technology Program of the Korea Institute of Energy Technology Evaluation and Planning (KETEP) granted financial resource from the Ministry of Trade, Industry and Energy, Republic of Korea (No. 20133030010930).

References and Notes

1. N. H. Como and A. M. Acevedo, *Sol. Energy Mater. Sol. Cells* 94, 62 (2010).
2. S. Q. Hussain, S. Kim, S. Ahn, N. Balaji, Y. Lee, J. H. Lee, and J. Yi, *Sol. Energy Mater. Sol. Cells* 122, 130 (2014).
3. S. Q. Hussain, S. Kim, S. Ahn, H. Park, A. H. T. Le, S. Lee, Y. Lee, J. H. Lee, and J. Yi, *Met. Mater. Int.* 20, 565 (2014).
4. S. Q. Hussain, W. K. Oh, S. Ahn, A. H. T. Le, S. Kim, Y. Lee, and J. Yi, *Vacuum* 101, 18 (2014).
5. M. G. Mason, L. S. Hung, C. W. Tang, and M. Wang, *J. Appl. Phys.* 86, 1688 (1999).
6. S. H. Kim, J. S. Jang, and J. Y. Lee, *Appl. Phys. Lett.* 89, 253501 (2006).
7. C. C. Wu, C. I. Wu, J. C. Strum, and A. Kahn, *Appl. Phys. Lett.* 70, 1348 (1997).
8. R. Schlaf, H. Murata, and Z. H. Kafafi, *J. Electron Spectrosc. Rel. Phenom.* 120, 149 (2001).
9. Y. Park, V. Choong, and Y. Gao, *Appl. Phys. Lett.* 68, 2699 (1996).
10. A. Nakasa, M. Adachi, E. Suzuki, and H. Usami, *Thin Solid Films* 484, 272 (2005).
11. W. K. Oh, S. Q. Hussain, Y. J. Lee, Y. Lee, S. Ahn, and J. Yi, *Mater. Res. Bull.* 47, 3032 (2012).
12. S. Ahn, S. Kim, V. A. Dao, S. Lee, S. M. Iftiqar, D. Kim, S. Q. Hussain, and J. Yi, *Thin Solid Films* 546, 342 (2013).
13. S. Lee, S. J. Tark, C. S. Kim, D. Y. Jeong, and D. Kim, *Curr. Appl. Phys.* 13, 836 (2013).
14. D. Rached and R. Mostefaoui, *Thin Solid Films* 516, 5087 (2008).
15. E. Centurioni and D. Iencinella, *IEEE Electron Device Lett.* 24, 177 (2003).
16. T. Minami, T. Miyata, and T. Yamamoto, *Surf. Coat. Technol.* 108-109, 583 (1998).
17. T. Minami, *J. Vac. Sci. Technol. A* 17, 1765 (1999).
18. D. S. Ginley, H. Hosono, and D. C. Paine, *Handbook of Transparent Conductors*, Springer, New York (2010).
19. S. K. So, W. K. Choi, C. H. Cheng, L. M. Leung, and C. F. Kwong, *Appl. Phys. A* 68, 447 (1999).
20. J. Seol, M. L. Monroe, T. J. Anderson, M. A. Hasnain, and C. Park, *IEEE* 236 (2006).
21. S. T. Hwang and C. B. Park, *Trans. Electr. Electron. Mater.* 11, 81 (2010).
22. B. Zhang, *Mater. Sci. Semi. Proc.* 13, 411 (2010).
23. Y. L. Lee and K. M. Lee, *Trans. Electr. Electron. Mater.* 10, 203 (2009).
24. S. Li and X. Qiao, *J. Chen, Mater. Chem. Phys.* 98, 144 (2006).
25. B. Zhang, X. Dong, X. Xu, and P. Zhao, *Sol. Energy Mater. Sol. Cells* 92, 1224 (2008).
26. H. C. Lee and O. O. Park, *Vacuum* 80, 880 (2006).
27. W. Deng, T. Ohgi, H. Nejo, and D. Fujita, *Jpn. J. Appl. Phys.* 40, 3364 (2001).
28. S. Cho, *Trans. Electr. Electron. Mater.* 10, 185 (2009).

Received: 10 July 2013. Accepted: 1 April 2014.